Journal of Biomolecular Structure and Dynamics
iFirst, 2012, 1–10

Steered molecular dynamics simulations on the binding of the appendant structure and helix-β2 in domain-swapped human cystatin C dimer

Manli Shen[a,b], Jing Guan[a], Linan Xu[a], Yuanyuan Yu[a], Jianwei He[a], Gary W. Jones[c] and Youtao Song[a,b]*

[a]*Province Key Laboratory of Animal Resource and Epidemic Disease Prevention, Liaoning University, Shenyang 110036, China;* [b]*School of Environmental Science, Liaoning University, Shenyang 110036, China;* [c]*Department of Biology, National University of Ireland Maynooth, Maynooth, County Kildare, Ireland*

Communicated by Ramaswamy H. Sarma

(*Received 8 January 2012; final version received 5 April 2012*)

We have performed steered molecular dynamics (SMD) simulations to investigate the dissociation process between the appendant structure (AS) and helix-β2 in human cystatin C dimer. Energy change during SMD showed that electrostatic interactions, including hydrogen bonds and salt bridges, were the dominant interactions to stabilize the two parts of the dimer. Furthermore, our data indicated that residues, Asn35, Asp40, Ser44, Lys75, and Arg93 play significant roles in the formation of these electrostatic interactions. Docking studies suggested that the interactions between AS and β2-helix were formed following domain swapping and were responsible for stabilizing the structure of the domain-swapped dimer.

Keywords: human cystatin C; steered molecular dynamics; appendant structure; amyloid; domain swapping

Introduction

More than 40 proteins have been identified as forming domain-swapped configurations, among such proteins are the prion protein, interleukin-10, p13suc1 and cystatins (Knaus et al., 2001; Rousseau, Schymkowitz, Wilkinson, & Itzhaki, 2001; Staniforth et al., 2001; Zdanov et al., 1995). The conversion of monomeric proteins to oligomers through domain swapping has been proposed as one possible early-stage mechanism underlying amyloid fibril formation (Yang, Levine, & Onuchic, 2005). Domain-swapped proteins display diverse primary amino acid sequences and secondary structures in the swapped regions, as well as flexibility and diversity in the hinge regions. Human cystatin C (hCC) was the first disease-causing amyloidogenic protein whose oligomerization was shown to be dependent on domain swapping (Janowski et al., 2001; Staniforth et al., 2001). Recent experiments on hCC have shown that prevention of domain swapping inhibits amyloid fibrils by up to 80% (Nilsson et al., 2004). The native structure of each cystatin molecule consists of a long central helix wrapped around a five-stranded anti-parallel β-sheet. The connectivity within the β-strands is: (N)-β1-(α)-β2-L1-β3-(AS)-β4-L2-β5-(C), where AS is a broad "appendant structure" unrelated to the compact core of the molecule and positioned on the opposite end of the β-sheet relative to the N-terminus and loops L1 and L2 (Jaskolski, 2001). Prior to oligimerization, the original monomer exchanges β1-(α)-β2 domain with the other, forming a hybrid dimer structure, which is the basic unit of pathogenic amyloid fibrils. Each subunit of the dimer is composed of the β1-(α)-β2 domain contributed by one molecule and the β3-(AS)-β4-β5 domain contributed by the other protein (Wahlbom et al., 2007). Such large-scale structural rearrangements arise from the unfolding of the original native structure of the monomer and the refolding of the hybrid structure.

The transient interactions and atomic-level dictating dimer formation are difficult to assess using current biophysical methods. Recently computational approaches have provided insight into this process. Molecular dynamics (MD) studies on the unfolding of the mutated cystatin monomer before dimerization showed that the L68Q variant, located in the hydrophobic core, caused destabilization of the molecular α/β dimer interface. This destabilization led to structural rearrangements that resulted in a higher propensity for partial unfolding of monomers (Calero et al., 2001; Sanders et al., 2004). A

*Corresponding author. Email: ysong@lnu.edu.cn

ISSN 0739-1102 print/ISSN 1538-0254 online

http://dx.doi.org/10.1080/07391102.2012.689698
http://www.tandfonline.com

recent study also suggested an analogous domain swapping process, propagating in an open-ended fashion, as being the underlying mechanism for cystatin's ability to form amyloid fibrils (Janowski et al., 2001). However, the exact mechanism of the dynamic process of dimer formation from unfolded cystatin monomers has yet to be elucidated.

Classical MD methods are mainly applied to simulate systems under conditions of equilibrium, while applying such methods to systems not in equilibrium (such as domain swapping) requires immense computational power and is extremely time consuming (Orzechowski & Cieplak, 2005; Zhang, Tan, Lim, & Tay, 2006). Steered molecular dynamics (SMD) was first introduced by Grubmuller et al., and is a way to computationally mimic the use of an atomic force microscope (AFM) to assess the interactions between two objects (Zhang et al., 2010b). A major application of SMD is in studying ligand-receptor and/or protein-protein dissociation by applying time-dependent external forces to the system. Assessment of changes in a variety of interactions between molecules in the system can provide detailed insight into atomic level changes that occur in response to external stimuli (Grubmuller, Heymann, & Tavan, 1996). We reasoned therefore that SMD simulations could be applied to provide insight into the process of domain-swapped cystatin dimer formation by molecular analysis of the reverse process, namely the unfolding of the dimeric form back to the monomeric form.

According to the hCC dimer 3D structure interactions between monomers occur through two major interaction regions: side regions formed by the AS and part of helix-β2 and central regions formed by the β3 and β2 helices (Su & Wang, 2009). The binding of AS and helix-β2 acts as a "clothespin" to fix the two sides of cystatin dimer. In previous studies from our group, we showed that the structure of the AS of chicken cystatin showed obvious deviations and distortions compared to two monomeric amyloid-forming mutants (I66Q and I108T). This suggested that the AS plays an important role in cystatin dimerization and amyloid formation, prior to domain swapping (Yu et al., in press, 2010). In order to further investigate the role of the AS in cystatin dimerization and amyloid formation, we performed SMD simulations whereby the AS was dissociated from helix-β2 in the hCC dimer under constant velocity. The conformational changes during dissociation were explored by assessment of crucial associations between amino acid residues interacting at the AS and helix-β2 interface. Analysis of interaction energy, hydrogen bonding and salt bridge formation, allows identification of the key residues in the monomers that are predicted to interact in dimer formation. This work provides insight into the molecular interactions and important amino acid residues that play a key role in the formation of hCC dimer and therefore underpin the eventual formation of amyloid fibrils.

Materials and methods

Model construction

The model of the hCC dimer molecule used in our study was constructed according to the X-ray crystal structure and coordinates of hCC dimer (PDB ID: 1TIJ), which were obtained from RCSB protein data bank (Su & Wang, 2009). The model of the hCC monomer molecule used in our docking work was constructed using homologous modeling methodology through the online service of Swiss Model (http://swissmodel.expasy.org/) (Janowski, Kozak, Abrahamson, Grubb, & Jaskólski, 2005), which was based on the crystallographic structure of a stable mutant of hCC V57 N (PDB ID: 3NX0) (Orlikowska, Jankowska, Robert, Jaskolski, & Szyman ska., 2010).

MD and SMD simulations

The MD simulation was performed using the Gromacs 4.0 program (Hess, Kutzner, & Lindahl, 2008) at the Computer Center of Liaoning University on a dual-core Pentium 2.8G processor of Linux cluster. GROMOS96 43a1 (Bonvin, 2006) force-field parameters were used in all simulations in this study. The integration time-steps were 2 fs throughout the whole simulation. The short-range non-bonded interactions were defined as van der Waals (VDW) and electrostatic interactions between particles within 0.9 nm. Long-range electrostatic interactions were calculated with the particle mesh Ewald method (Darden, York, & Pedersen, 1993) with a maximum fast-Fourier transforms (FFT) grid spacing of 0.12 nm and cubic interpolation order. Periodic boundary conditions were activated in the simulations. Bonds containing hydrogen atoms were constrained using the SHAKE algorithm with a relative tolerance of 10^{-5} Å. The dimeric hCC model was solvated in a water box containing 10124 SPC216 water molecules (Berendsen, Postma, van Gunsteren, & Hermans, 1981) and neutralized by adding 2 Cl^- counter ions. The cubic box side was $20 \times 20 \times 20\ nm^3$. The solvated and neutralized systems were then energy-minimized for 20 ps. Afterwards, the backbone atoms of the structure were fixed, while the side chains and solvent were allowed to move under minimal restraint for further 10 ps, followed by totally unrestrained equilibration for 12 ps, at a constant temperature of 300 K and 1 atm pressure within a water box using periodic boundary conditions in the Isobaric-Isothermal (NPT) ensemble. Following equilibration the productive run was carried out over 3 ns with the temperature kept constant at 300 K, and pH7. In all simulations the temper-

ature was maintained close to the intended values by weak coupling to an external temperature bath with a coupling constant of 0.1 ps. The protein and the rest of the system were coupled separately to the temperature bath.

SMD simulations with constant velocity were then performed. In this process, keeping the mass center of helix-β2 region (residues Lys36 to Ala46) fixed, external steering forces were applied to the reference point (the mass center of AS-β3, i.e. residues Thr71 to Arg93) to pull the AS domain along the predefined direction (Figure 1). During the SMD simulations, the force was only applied along the pulling direction. Based on the 3D structure of hCC dimer and the hypothetical domain swapping mechanism, the pulling direction in the system was assigned on all hydrogen bonding contributor pairs between the pull regions for effective separation of the AS. The trajectories were saved for every 0.5 ps, and steering forces were recorded every 10 fs. Each trajectory along the same pathways was repeated three times.

Automated docking

Molecular docking was performed using Hex package (Ritchie & Kemp, 2000) to investigate the possible interactions between two hCC monomers. During the whole process, the two molecules were kept rigid. Hex generates a diversified set of conformations by making random changes of the coordinates of two molecules using spherical polar Fourier algorithm (Kabsch & Sander, 1983) within a specified box. The most favorable conformation with the highest energy score of each substrate was selected for comparison.

Analysis of the trajectories and interaction energy calculation

The secondary structure of the protein was determined using the DSSP program (Humphrey, Dalke, & Schulten, 1996). Visual molecular dynamics (Kabsch & Sander, 1983) and the LigPlot program (Wallace, Laskowski, & Thornton, 1995) with appropriately developed original scripts were used for system visualization and analysis. The root mean square deviations (RMSD) were calculated for all α-carbon atoms with reference to the first frame of the trajectories. To examine the energetic properties of hydrogen bond, salt bridge and VDW during the unbinding process, hCC conformation at different times of the SMD trajectory was recorded. Their relative energies were computed using the electronic correlation quantum mechanics method Moller–Plesset second order perturbation (MP2) (Pople & Head-Gordon, 1988) and carried out using Gromac 4.0 software.

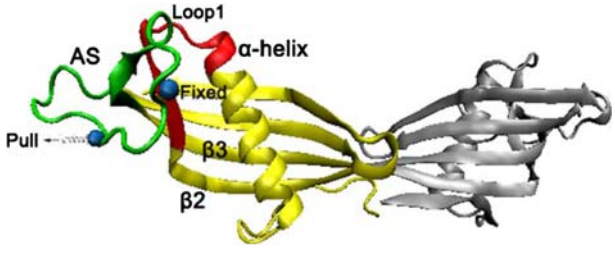

Figure 1. Ribbon schematic representation of the hCC dimer. The pulling region of AS-β3 and fixed region of helix-β2 are highlighted with green and red, respectively. The blue balls are the mass center of the Cα atoms, to which the fixed and harmonic potential is assigned. The spring arrow indicates the direction of pull of the AS in the SMD simulations.

Results and discussion

MD equilibrium simulation

To equilibrate interaction regions before performing the SMD simulations, a 3 ns MD simulation of the fully solvated hCC dimer was carried out at pH 7 and 300 K. The structural stability of hCC was assessed by calculation of the RMSD. The overall RMSD of the whole system, as well as Cα atoms of the protein, indicated that the conformation of the protein appeared to be equilibrated shortly after the beginning of simulation and the values of RMSD were generally stabilized at 0.45 and 0.40 nm for all atoms and Cα atoms, respectively (Figure 2). The stable structure of the protein provided a basal starting point for the subsequent SMD simulations.

Determination of the pulling velocity and spring constant

Based on the 3D structure of the hCC dimer and the hypothetical domain swapping mechanism, the pulling direction in the system was assigned to all hydrogen bonding contributing pairs to effectively pull the AS

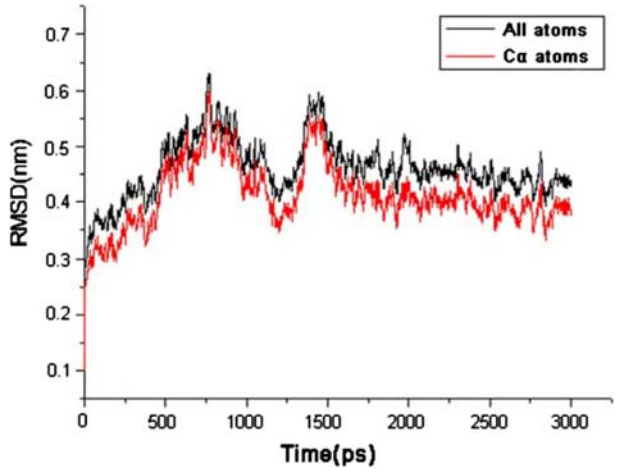

Figure 2. Time dependence of the RMSD from the crystal structure of hCC dimer for the Cα (red) and all atoms (black) in the 3 ns equilibrium MD simulation.

away from helix-β2 region. Considering the flexibility of the AS and the relative stability of helix-β2 region, the mass center of the helix-β2 region was chosen as the fixed region. In constant velocity SMD (cv-SMD), the value of spring force varied significantly depending on different pulling velocities and spring constants. A previous study has shown that higher pulling velocities lead to dis-equilibrium and may introduce errors into the simulation results (Isralewitz, Gao, & Schulten, 2001). To avoid inducing experimental errors in the system and in accordance with AFM experimentation, the pulling velocity should be as small as possible (Zhang et al., 2010b). To choose a suitable velocity for the hCC dimer system, we carried out eight simulations each employing a different pulling velocity; ranging from 0.003 to 0.08 nm/ps. Figure 3(A) summarizes the results of the rupture forces caused by difference in this range of pulling velocities. There was an apparent linear dependency between the rupture force and the pulling velocity when velocities were lower than 0.05 nm/ps (Figure 3(A)). For subsequent SMD simulations we chose a pulling velocity of 0.003 nm/ps as the external harmonic potential appears to have no influence on the structure of the AS.

In choosing a spring constant to be used in the SMD simulation two major factors need to be considered; the spring constant must be high enough to enable the local unbinding potential to be determined, but it must not be so high as to make the measured force be masked by background noise (Zhang et al., 2010b). To choose an appropriate spring constant we performed six simulations with varying spring constants being applied and these ranged from 100 to 4000 kJ/mol/nm^2 (Figure 3(B)). The results showed that under the same pulling velocity smaller spring constants produced a delay in the maximum force value and peaks became more distinct (Figure 3(B)). Spring constants of 1000–4000 kJ/mol/nm^2 produced large fluctuations in the intensity of peaks and in background noise made it impossible to accurately measure the force (Figure 3(B)). In contrast spring constants of 100 and 250 kJ/mol/nm^2 failed to produce enough fluctuation in peak intensity, which suggested that these spring constants were not enough to ensure the validity of the stiff-spring approximation for the guiding potential (Figure 3(B)). A spring constant of 500 kJ/mol/nm^2 produced measurable and reliable peak fluctuations with minimal background noise (Figure 3 (B)) and was thus chosen for the subsequent SMD simulations.

Conformational changes of the hCC dimer

According to the RMSD values of SMD simulation, obvious conformational changes in the hCC dimer were observed during the dissociation process (Figure 4(A)). Figure 4(B) (left) shows the original structure of hCC dimer after 3 ns of MD. At this stage seven hydrogen bonds (blue) were detected between residues Thr71, Cys73, Lys75, Arg93 located in the AS (green) and residues His43, Met41, Asn35, Ser38 located in helix-β2 of the other monomer (red). This hydrogen bond network is responsible for the structural stability of the cystatin dimer. After 1 ns of the SMD simulation, the AS apparently shifts from its original location onto the helix-β2 side (Figure 4(B), right). The distances between the mass center (Pro84) of the AS and the mass center (His43) of helix-β2 before and after pulling were 1.03 and 1.44 nm, respectively. Due to the pulling direction applied to the system to ensure effective separation of the AS, all seven hydrogen bonds between residues in the AS and those in helix-β2 regions disappeared (Figure 4(B)). This indicated that the AS was completely pulled away from helix-β2 and the hydrogen-bonded network was clearly disrupted in this process.

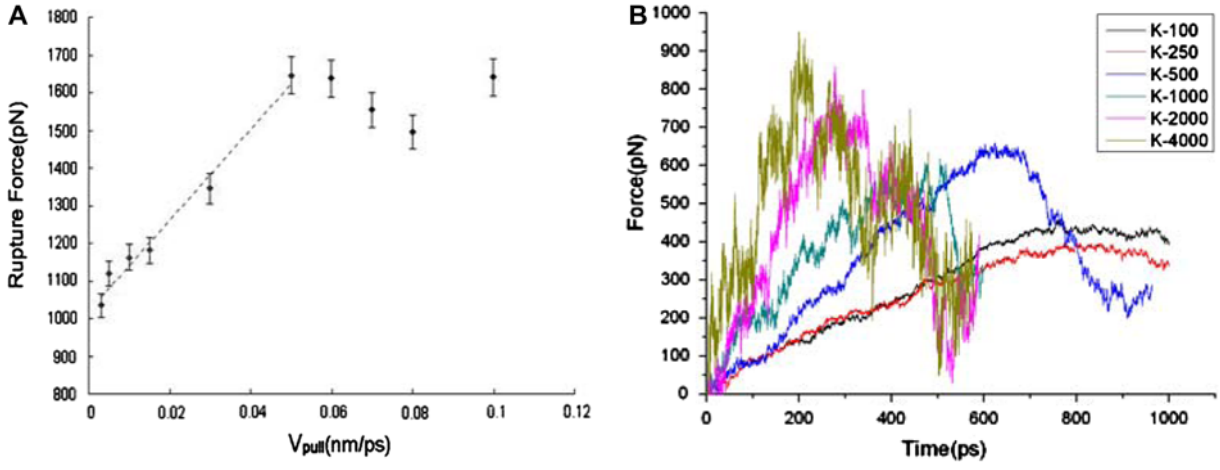

Figure 3. (A) Computed rupture forces as a function of pulling velocity V_{pull}. The error bars give an estimated uncertainty. The dashed line shows a linear fit to the computed forces for V_{pull} less than 0.05 nm/ps. (B) Influence of different spring constants on the steering force of the dimer.

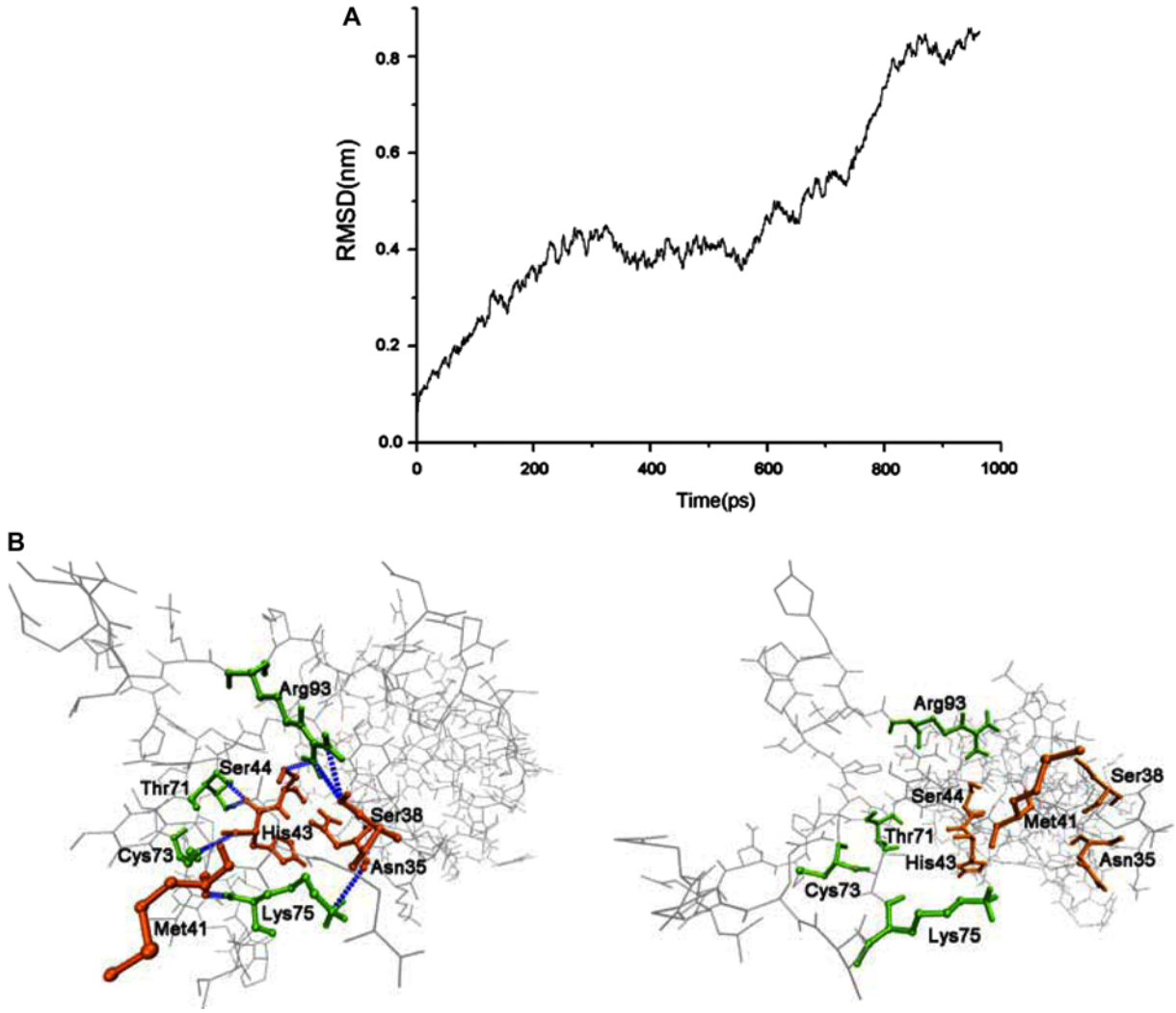

Figure 4. (A) RMSD value by the Cα atoms of hCC during SMD with external forces being applied. (B) Changes observed in the structure of AS and helix-β2 regions after SMD simulation. The positions of the related residues in the original structure with hydrogen bonds are shown in the left panel. The positions of the related residues after non-equilibration are shown in the right panel. Other residues are presented through gray lines. Blue dashed lines represent hydrogen bonds.

Energy analysis of the dissociation process

The dissociation of the AS from helix-β2 is a dynamic procedure, which can be determined by the lowest free energy state. Upon commencement of the SMD simulation the system shifts into a state of dis-equilibrium. During this transition the changes in interaction energy between the pulling regions were assessed during the dissociation process. As shown in Figure 5(A), the predominant interactions contributing to total interaction energy were electrostatic with VDW interactions having less of an impact. The starting point of the curve corresponds to the most thermodynamically stable state with the lowest free energy. Due to the effect of the steering force, the system began to be in a dis-equilibrium state after the data point. With the time lapse, the curve of the interaction energy decreased, which indicated that there were strong interactions present between the AS and helix-β2 during this dynamic process. The interactions increased to the maximum when the energy reached the lowest point. After 700 ps, the AS gradually shifted from the helix-β2 region and the energy curve quickly drops to zero with minor fluctuations (Figure 5(A)). To determine the role of related residues in the pulling region, we analyzed the electrostatic interactions among residues in this hydrogen-bonded network at the lowest point of energy. The interaction energies of these residues during the steered phase are shown in Figure 5(B). The major fluctuations observed in the interaction energy map for residues Lys75 and Arg93 demonstrate that these residues play significant roles during the dissociation process

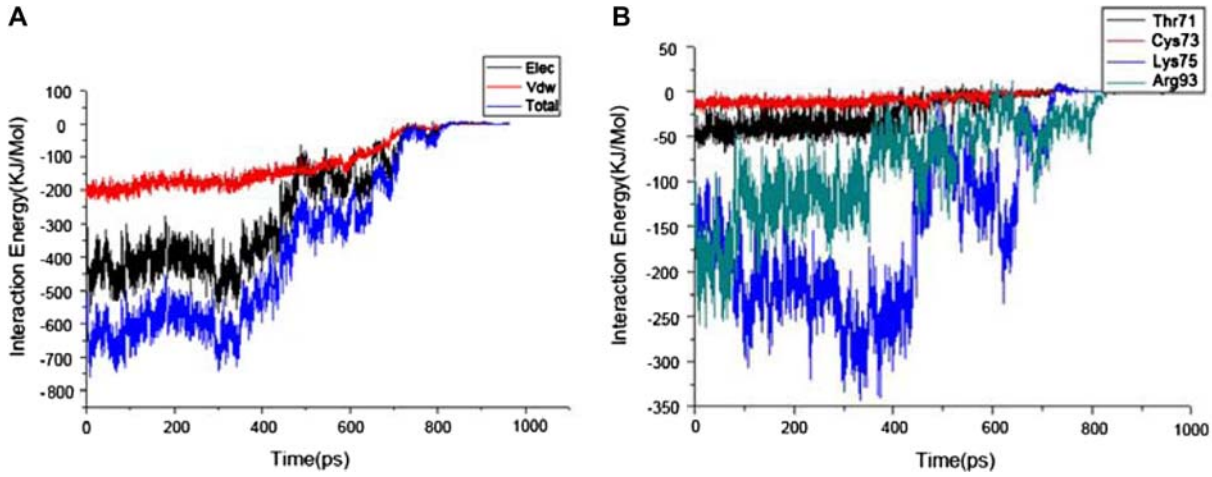

Figure 5. Time dependence of the interaction energy between the AS and helix-β2 regions (A) and (B) the related residues during the SMD simulation.

with respect to critical interactions between the AS and helix-β2. In contrast the energy plots for Thr71 and Cys73 suggest that these residues have far less of an impact on the dissociation process. Furthermore, the overall interaction energy analysis of the pulling region indicated equal influence of residues located at the right and left side of the hCC dimer suggesting a symmetric structure in these regions (12 and data not shown).

Analysis of hydrogen bonding status during the dissociation process

Hydrogen bonds are the most abundant type of non-covalent interactions and are important in stabilizing protein structures. Previous analysis of the hCC dimer crystal structures assessed and characterized extensive electrostatic interactions between a slice of β3-AS and part of helix-β2 region (Zhang et al., 2010a). The existence of the inter-chain hydrogen bonds between important amino acids in AS and helix-β2 during dissociation process was determined (Figure 6(A)). The results indicated that hydrogen bonds C73 (O)–H43 (H), K75 (NZ) –N35 (O), T71 (OG1) –H43 (O), T71 (N) –H43 (O) and R93 (NH1)–S44 (OG) were all relatively stable during the SMD simulations. To estimate the strength of these hydrogen bonds, we further analyzed the interaction energy of the five hydrogen bonds listed above (Figure 6(B)). Compared to other interactions the hydrogen bond energy of K75/N35 showed dramatic fluctuation during the simulation, suggesting that this played an important role in intermolecular interactions. These data were in agreement with the data obtained for interaction energies (Figure 5(B)). Interestingly, the hydrogen bond energy of R93/S44 showed only minor fluctuation during the simulation but the overall interac-

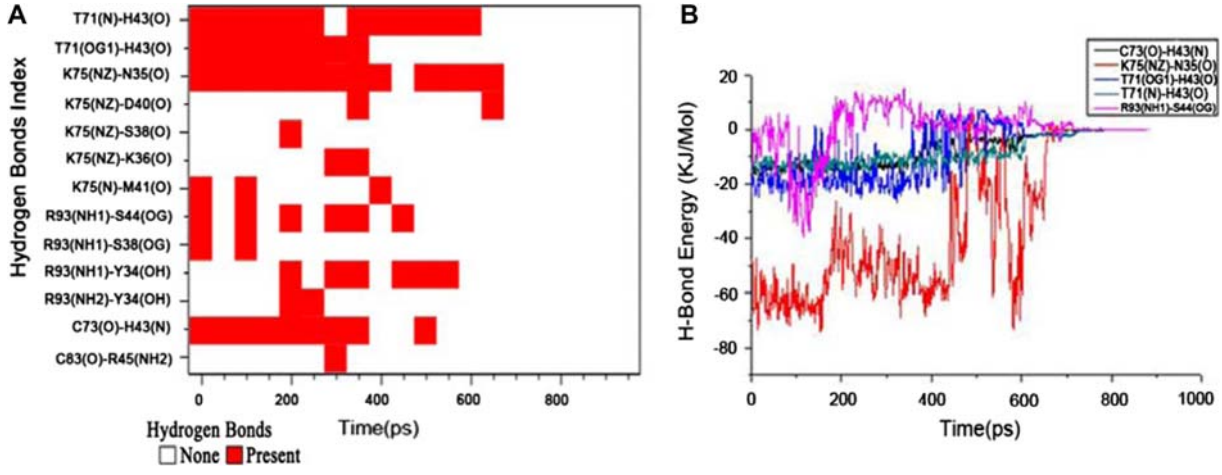

Figure 6. (A) Existence of hydrogen bonds between the AS and helix-β2 regions during SMD simulation. (B) Energy analysis of selected hydrogen bonds during SMD simulation.

tion energy of residue Arg93 was similar to that of Lys75 during the steered phase, suggesting that Arg93 may also form other important interactions as well as hydrogen bonds (see next section). The impact of residues Thr71 and Cys73 seems less significant in the dissociation process.

Analysis of salt bridge formation during the dissociation process

Among the electrostatic interactions, salt bridges play a major role determining the tensile strength of protein–protein interactions. We evaluated the electrostatic interactions by calculating the distances between all charged groups in the pulling region. Based upon previously published data, if the distance between two oppositely charged residues came within 0.4 nm this was defined as a salt bridge (Tiberti & Elena, 2011). Figure 7 summarizes the important salt bridges formed during the dissociation process. Only one salt bridge was detected during the simulation, formed between Arg93 in the AS and Asp40 in loop1, directly connected to the strands on the loop binding site, which was important in stabilizing the structure. This electrostatic interaction was particularly stable because of the low dielectric environment in the interior of the AS and loop1. The salt bridge formed by Arg93 contributes to the overall interaction energy of this residue and clarifies why the overall interactions energies of Arg93 and Lys75 are similar.

Proposed roles for residues Lys75, Arg93, Asn35, Ser44 and Asp40 in cystatin dimerization

Our SMD study has identified interactions between residues Lys75, Arg93 (located in the AS) and Asn35, Ser44, Asp40 (located in helix-β2) as having significant effects on stabilization of the dimeric structure of hCC. Within the hCC dimer the monomers appear to interact to form a "clothespin"-type structure fixed through a variety of electrostatic interactions. To investigate whether this "clothespin" structure fixes the two monomers and promotes domain swapping we carried simulated docking experiments between two hCC monomers. The docking structure that had the highest score (lowest total docking energy) was selected for further analysis. This structure showed that the distances between the residues implicated in dimer stabilization were too far to form intermolecular interactions ($Distance_{K75/N35} = 3.73$ nm, $Distance_{R93/S44} = 4.21$ nm, $Distance_{R93/D40} = 4.26$ nm) (Figure 8(A)). Subsequently ten other high-scoring docking structures were assessed and showed similar results (data not shown). In addition, these docking results also indicated that existing interacting regions of the AS and β2-helix in different monomers were also distant (Figure 8(B)), and did not correspond to the structural data of hCC following SMD simulations (Figures 4(B) and 8(C)). This strongly suggests that interactions between the AS and β2-helix were formed after domain swapping and are responsible for stabilizing the domain-swapped dimer structure rather than promoting domain swapping. Additionally, one interesting finding from our docking studies is the hydrogen bond formed between Asn82 and Lys54 of hCC monomers (Figure 8). Given the location of these hydrogen bonds at extreme ends of the initially formed dimer interface, it is an intriguing possibility that these interactions are key players in "fixing" the monomers in place prior to domain swapping and amyloid formation.

This SMD simulations study has identified key residues and interactions that are predicted to play a signifi-

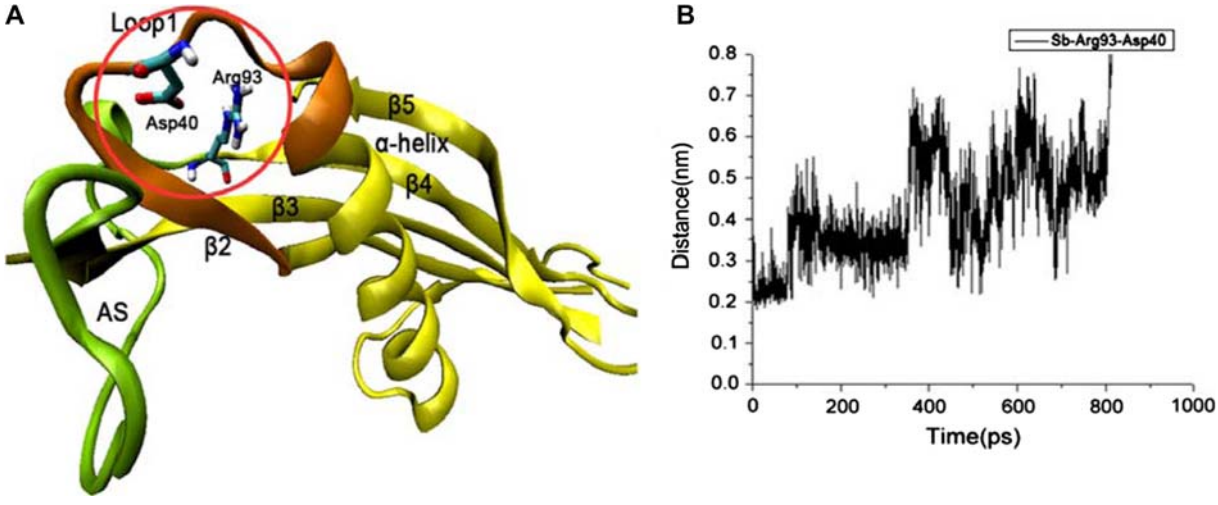

Figure 7. (A) Interaction site of the salt bridge Arg93-Asp40 which stabilizes the AS and helix-β2 regions in the original hCC structure. (B) The salt bridge distance between Arg93 and Asp40 as a function of SMD simulation time.

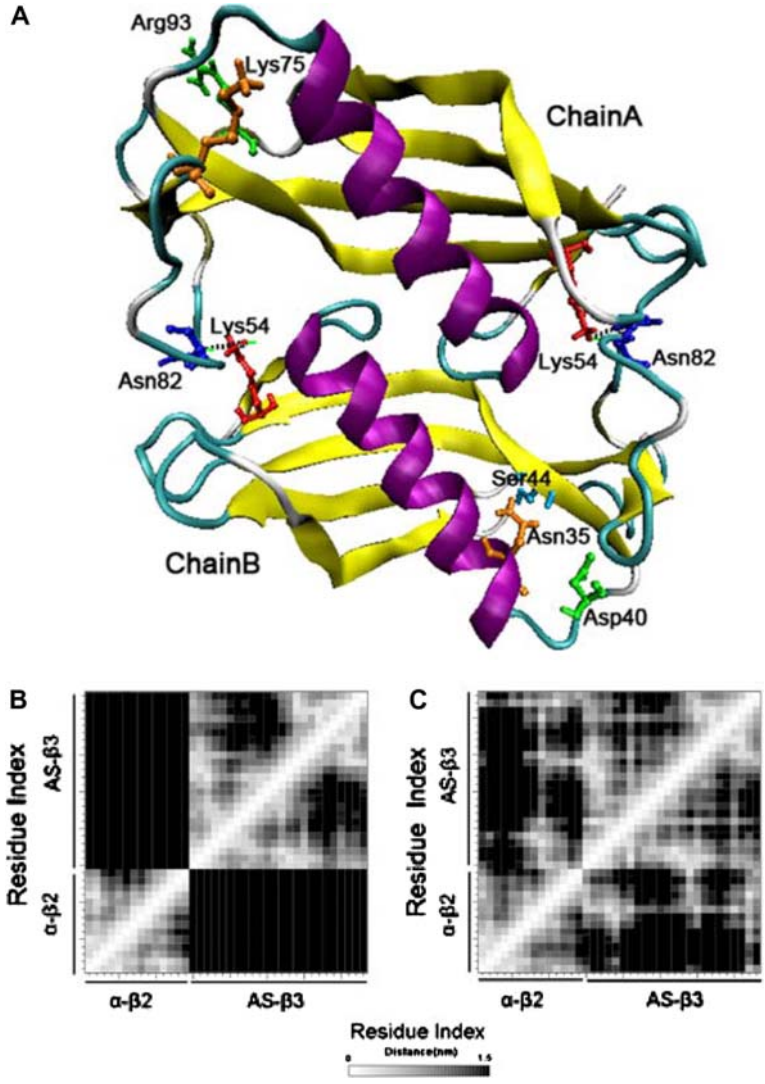

Figure 8. (A) Docking structure of two HCC monomers. Hydrogen bonds in the docking dimer were shown with blue dashed line. (B) Distance matrix of the AS and helix-β2 group between chains A and B in docking dimer. (C) Distance matrix of AS and helix-β2 group between chains A and B in steered hCC dimer.

cant role in the formation and stabilization of dimer formation by hCC. The fact the hCC dimer formation is a key step in the formation of amyloid fibrils by this protein means that the amino acids identified in this study may play a key role in the early molecular processes that result in hCC amyloid formation. In addition, to better understand hCC dimer destabilization following the SMD simulation, we attempted to perform a 5 ns reverse classical MD using the final structure of the SMD trajectory. However, the "re-formed" inter-chain hydrogen bonds between the AS and helix-β2 differ substantially from those identified during the SMD simulation, thus making such analysis difficult to assess (Data not shown). Such a destabilization study will require much longer simulation times and computational power. Nevertheless, our computational study provides new insights into the mechanism of domain swapping by hCC and provides a framework for the development of wet-lab experimentation for the assessment of appropriate hCC mutants and how amyloid formation may be influenced by alteration of the key residues highlighted in this study.

Abbreviations

SMD	steered molecular dynamics
AS	appendant structure
hCC	human cystatin C
AFM	atomic force microscope
RMSD	root-mean-square deviation.

Acknowledgments

This work was supported by grants from the National Natural Science Foundation of China (No. 30970152) and partially sponsored by the Fund of Liaoning Provincial Education Department (No. 2009R26). We are grateful to Yuan Yu and Mengyuan Zhang for technical assistance in MD simulations. We thank Prof. Dongqing Wei of Shanghai Jiaotong University for his kind support and helpful discussion.

References

Berendsen, H.J.C., Postma, J.P.M., van Gunsteren, W.F., & Hermans, J. (1981). Interaction models for water in relation to protein hydration. In B. Pullman (Ed.), *Intermolecular forces* (pp. 331–342). Dordrecht: D Reidel.

Bonvin, A.M. (2006). Flexible protein–protein docking. *Current Opinion in Structural Biology, 16*, 194–200.

Calero, M., Pawlik, M., Soto, C., Castano, E.M., Sigurdsson, E.M., Kumar, A., … Levy, E. (2001). Distinct properties of wildtype and the amyloidogenic human cystatin C variant of hereditary cerebral hemorrhage with amyloidosis. *Icelandic Type. Journal of neurochemistry, 77*, 628–637.

Darden, T., York, D., & Pedersen, L. (1993). Particle mesh Ewald: An N∗log(N) method or Ewald sums in large systems. *Journal of Chemical Physics, 98*, 10089–10092.

Grubmuller, H., Heymann, B., & Tavan, P. (1996). Ligand binding: Molecular mechanics calculation of the streptavidin biotin rupture force. *Science, 271*, 997–999.

Hess, B., Kutzner, C., & Lindahl, E. (2008). GROMACS 4: Algorithms for highly efficient, load-balanced, and scalable molecular simulation. *Journal of Chemical Theory and Computation, 4*, 435–447.

Humphrey, W., Dalke, A., & Schulten, K. (1996). VMD – visual molecular dynamics. *Journal of Molecular Graphics, 14*, 33–38.

Isralewitz, B., Gao, M., & Schulten, K. (2001). Steered molecular dynamics and mechanical functions of proteins. *Current Opinion in Structural Biology, 11*, 224–230.

Janowski, R., Kozak, M., Abrahamson, M., Grubb, A., & Jaskólski, M. (2005). 3D domain swapped human cystatin C with amyloidlike intermolecular beta-sheets. *Proteins, 61*, 570–578.

Janowski, R., Kozak, M., Jankowska, E., Grzonka, Z., Grubb, A., Abrahamson, M., & Jaskolski, M. (2001). Human cystatin C, an amyloidogenic protein, dimerizes through three-dimensional domain swapping. *Natural Structural Biology, 8*, 316–320.

Jaskolski, M. (2001). 3D Domain swapping, protein oligomerization, and amyloid formation. *Acta Biochimica Polonica, 48*, 807–827.

Kabsch, W., & Sander, C. (1983). Dictionary of protein secondary structure: Pattern recognition of hydrogen-bonded and geometrical features. *Biopolymers, 22*, 2577–2637.

Knaus, K.J., Morillas, M., Swietnicki, W., Malone, M., Surewicz, W.K., & Yee, V.C. (2001). Crystal structure of the human prion protein reveals a mechanism for oligomerization. *Natural Structural Biology, 8*, 770–774.

Nilsson, M., Wang, X., Rodziewicz-Motowidlo, S., Janowski, R., Lindstrom, V., Onnerfjord, P., … Grubb, A. (2004). Prevention of domain swapping inhibits dimerization and amyloid fibril formation of Cystatin C. *Journal of Biological Chemistry, 279*, 24236–24245.

Orlikowska, M., Jankowska, E., Robert, K., Jaskolski, M., & Szyman ska., A. (2010). Hinge-loop mutation can be used to control 3D domain swapping and amyloidogenesis of human cystatin C. *Journal of Structural Biology, 173*, 406–413.

Orzechowski, M., & Cieplak, P. (2005). Application of steered molecular dynamics (SMD) to study DNA–drug complexes and probing helical propensity of amino acids. *Journal of Physics: Condensed Matter, 17*, 1627–1640.

Pople, J.A., & Head-Gordon, M. (1988). MP2 energy evaluation of direct methods. *Chemical Physics Letters, 153*, 503–506.

Ritchie, D.W., & Kemp, G.J. (2000). Protein docking using spherical polar Fourier correlations. *Proteins, 39*, 178–194.

Rousseau, F., Schymkowitz, J.W.H., Wilkinson, H.R., & Itzhaki, L.S. (2001). Three-dimensional domain Protein Oligomerization through Domain Swapping 209 swapping in p13suc1 occurs in the unfolded state and is controlled by conserved proline residues. *Proceedings of the National Academy of Sciences, 98*, 5596–5601.

Sanders, A., Jeremy Craven, C., Higgins, L.D., Giannini, S., Conroy, M.J., Hounslow, A.M., … Staniforth, R.A. (2004). Cystatin forms a Tetramer through Structural rearrangement of domain-swapped dimers prior to Amyloidogenesis. *Journal of Molecular Biology, 336*, 165–178.

Staniforth, R.A., Giannini, S., Higgins, L.D., Conroy, M.J., Hounslow, A.M., Jerala, R., … Waltho, J.P. (2001). Three dimensional domain swapping in the folded and molten-globule states of cystatins, an amyloid-forming structural superfamily. *EMBO Journal, 20*, 4774–4781.

Su, Z.Y., & Wang, Y.T. (2009). A molecular dynamics simulation of the human Lysozyme – Camelid VHH HL6 antibody system. *International Journal of Molecular Sciences, 10*, 1719–1727.

Tiberti, M., & Elena, P. (2011). Dynamic properties of extremophilic subtilisin-like serine-proteases. *Journal of Structural Biology, 174*, 69–83.

Wahlbom, M., Wang, X., Lindstrom, V., Carlemalm, E., Jaskolski, M., & Grubb, A. (2007). Fibrillogenic oligomers of human cystatin C are formed by propagated domain swapping. *Journal of Biological Chemistry, 282*, 18318–18326.

Wallace, A.C., Laskowski, R.A., & Thornton, J.M. (1995). LIGPLOT: A program to generate schematic diagrams of protein-ligand interactions. *Protein Engineering, 8*, 127–134.

Yang, S., Levine, H., & Onuchic, J.N. (2005). Protein oligomerization through domain swapping: Role of inter-molecular interactions and protein concentration. *Journal of Molecular Biology, 352*, 202–211.

Yu, Y, Liu, X., He, J., Zhang, M., Li, H., Wei, D., & Song. Y. (in press). Appendant structure plays an important role in amyloidogenic cystatin dimerization prior to domain swapping. *Journal of Biomolecular Structure & Dynamics*.

Yu, Y., Wang, Y., He, J., Liu, Y., Li, H., Zhang, H., & Song, Y. (2010). Structural and dynamic properties of a new amyloidogenic chicken cystatin mutant I108T. *Journal of Biomolecular Structure & Dynamics, 27*, 641–649.

Zdanov, A., Schalk-Hihi, C., Gustchina, A., Tsang, M., Weatherbee, J., & Wlodawer, A. (1995). Crystal structure of interleukin-10 reveals the functional dimer with an unexpected topological similarity to interferon γ. *Structure, 3*, 591–601.

Zhang, B., Su, Z., Tay, T.E., & Vincent, B.C.T. (2010a). Mechanism of CDK5 activation revealed by steered molecular dynamics simulations and energy calculations. *Journal of Molecular Modeling, 161*, 1159–1168.

Zhang, B., Tan, V.B.C., Lim, K.M., & Tay, T.E. (2006). Molecular dynamics simulations on the inhibition of cyclin-dependent kinases 2 and 5 in the presence of activators. *Journal of Computer-Aided Molecular Design, 20*, 395–404.

Zhang, J., Zheng, Q., & Zhang, H. (2010b). Unbinding of glucose from human pulmonary surfactant protein D studied by steered molecular dynamics simulations. *Chemical Physics Letters, 484*, 338–343.